

© 2023 IEEE. Personal use of this material is permitted. Permission from IEEE must be obtained for all other uses, in any current or future media, including reprinting/republishing this material for advertising or promotional purposes, creating new collective works, for resale or redistribution to servers or lists, or reuse of any copyrighted component of this work in other works.

D. Wang, H. Qi, B. Lian, Y. Liu and H. Song, "Resilient Decentralized Cooperative Localization for Multi-Source Multi-Robot System," in IEEE Transactions on Instrumentation and Measurement, doi: 10.1109/TIM.2023.3291805.

<https://doi.org/10.1109/TIM.2023.3291805>

Access to this work was provided by the University of Maryland, Baltimore County (UMBC) ScholarWorks@UMBC digital repository on the Maryland Shared Open Access (MD-SOAR) platform.

Please provide feedback

Please support the ScholarWorks@UMBC repository by emailing scholarworks-group@umbc.edu and telling us what having access to this work means to you and why it's important to you. Thank you.

Resilient Decentralized Cooperative Localization for Multisource Multirobot System

Dongjia Wang^{ID}, Huaiyuan Qi^{ID}, Baowang Lian^{ID}, Yangyang Liu^{ID}, and Houbing Song^{ID}, *Fellow, IEEE*

Abstract—Although cooperative localization (CL) is fundamental to multirobot systems, current algorithms suffer from the tracking of interdependencies, information fusion from multiple sources, and restriction to specific measurement models. To improve the accuracy of localization algorithms for multirobot systems and reduce the impact of uncertainty in multisource measurement information, this article proposes a resilient decentralized CL (RDCL) algorithm. We modify the measurement update procedure of the traditional decentralized CL (DCL) algorithm to track inter-robot correlations and ensure the independence of the measurement update procedure of the elemental filters. We use optimal information fusion algorithms to fuse multisource information, and determine the overall estimate of every robot through a weighted sum of multisource estimates, thereby achieving accurate localization. To enhance the robustness of the multirobot localization system, an online validation module is added to validate the multisource estimates. The proposed CL framework is decentralized and not restricted to specific models. Simulations results show that the proposed algorithm improves localization accuracy and resilience of the multirobot system compared to existing CL algorithms. Experimental results using real-world dataset demonstrate that our proposed algorithm can achieve a localization accuracy with an average root mean square error (ARMSE) of 0.68 m, and it is 34% better than that of the traditional DCL algorithm.

Index Terms—Cross correlation, decentralized cooperative localization (DCL), multirobot systems, multisource information fusion.

NOMENCLATURE

\mathbf{x}_k^i	State vector of robot i at time step k .
$\mathbf{f}_k(\cdot)$	Function of the state model of robot i .
\mathbf{u}_k^i	Control input of robot i .
\mathbf{w}_k^i	State noise of robot i .
\mathbf{Q}_k^i	Covariance matrix of state noise of robot i .
$\mathbf{z}_{p,k+1}^i$	Private measurement of robot i .

$\mathbf{h}_{p,k+1}^i$	Private measurement model of robot i .
$\mathbf{v}_{p,k+1}^i$	Private measurement noise of robot i .
$\mathbf{R}_{p,k+1}^i$	Covariance matrix of private measurement noise of robot i .
$\mathbf{z}_{r,k+1}^{ij}$	Relative measurement of robots i and j .
$\mathbf{h}_{r,k+1}^{ij}$	Relative measurement model of robots i and j .
$\mathbf{v}_{r,k+1}^{ij}$	Relative measurement noise of robots i and j .
$\mathbf{R}_{r,k+1}^{ij}$	Covariance matrix of relative measurement noise of robot i and j .
$[x_k^i, y_k^i]$	Position of robot i in the Cartesian coordinate system.
θ_k^i	Orientation of robot i .
V_k^i	Linear velocity of robot i .
ω_k^i	Rotational angular velocity of robot i .
$w_{V,k}^i$	Linear velocity noise of robot i .
$w_{\omega,k}^i$	Rotational angular velocity noise of robot i .
δt	Discretization time.
$d_{p,k+1}^{il}$	Range measurements of robot i to landmark l .
$\theta_{p,k+1}^{il}$	Bearing measurements of robot i to landmark l .
$v_{d_{p,k+1}^{il}}^i$	Range measurements noise of robot i to landmark l .
$v_{\theta_{p,k+1}^{il}}^i$	Bearing measurements noise of robot i to landmark l .
$d_{r,k+1}^{ij}$	Range measurements of robots i and j .
$\theta_{r,k+1}^{ij}$	Bearing measurements of robots i and j .
$v_{d_{r,k+1}^{ij}}^i$	Range measurements noise of robots i and j .
$v_{\theta_{r,k+1}^{ij}}^i$	Bearing measurements noise of robots i and j .
$\hat{\mathbf{P}}_k^i$	Covariance matrix of state estimate of robot i .
$\hat{\mathbf{P}}_k^{ij}$	Cross-covariances matrix of state estimate of robot i .
σ_k^{ij}	Half cross-covariances matrix of robot i .
\mathbf{F}_k^i	State Jacobi matrix of robot i .
\mathbf{G}_k^i	State noise Jacobi matrix of robot i .
\mathbf{H}_{k+1}^i	Measurement Jacobi matrix of robot i .
\mathbf{K}_{k+1}^i	Kalman gain of measurement of robot i .
$\mathbf{A}_{p,k+1}^i$	Weight of private measurement update.
$\mathbf{A}_{r,k+1}^i$	Weight of relative measurement update.
$\mathbf{A}_{j,k+1}^i$	Weight of the estimated received from other robots.
$L(\cdot)$	Objective function of Lagrange multiplier method.
λ	Lagrange multiplier.
L_{k+1}^i	Set of landmarks detected by robot i .

Manuscript received 28 February 2023; revised 3 June 2023; accepted 13 June 2023. Date of publication 3 July 2023; date of current version 13 July 2023. This work was supported in part by the National Natural Science Foundation of China under Grant 62171735, Grant 62173276, and Grant 62101458; and in part by the Natural Science Basic Research Program of Shaanxi under Grant 2021JQ-122. The Associate Editor coordinating the review process was Dr. George Dan Mois. (Corresponding author: Yangyang Liu.)

Dongjia Wang, Baowang Lian, and Yangyang Liu are with the School of Electronics and Information, Northwestern Polytechnical University, Xi'an 710129, China (e-mail: wangdongjia@mail.nwpu.edu.cn; bwlian@nwpu.edu.cn; liu_yang90@163.com).

Huaiyuan Qi is with Shaanxi Fenghuo Electronics Company Ltd., Baoji 721006, China (e-mail: huaiyuanqi@163.com).

Houbing Song is with the Department of Information Systems, University of Maryland, Baltimore County (UMBC), Baltimore, MD 21250 USA (e-mail: songh@umbc.edu; h.song@ieee.org).

Digital Object Identifier 10.1109/TIM.2023.3291805

- J_{k+1}^i Set of robots detected by robot i .
 T_{k+1}^i Number of estimates of robot i received from other robots.

I. INTRODUCTION

MULTIPLE robots forming a cooperative team can significantly improve the robustness and scalability of system; such teams also play a key role in tasks such as area surveillance, assisted navigation, and disaster management [1], [2], [3], [4]. Localization is regarded as one of the most fundamental tasks for multirobot systems. In contrast to localizing every robot independently, cooperative localization (CL) for multisource multirobot systems cooperatively estimates a robot's state through information sharing and utilizing its own observations and those of other robots [5], [6]. Every robot can obtain self-motion and relative measurements (e.g., range, bearing, relative pose, or any combination of them) through proprioceptive sensors and exteroceptive sensors [7], [8]. Although these relative observations may be noisy due to the limitations of exteroceptive sensors or environmental influences, they still provide information about the robot's state to compensate for the decreased localization performance caused by accumulated errors or failures of proprioceptive sensors [9]. Therefore, the multirobot CL method has major advantages over the independent localization method; it significantly improves the localization performance of individual robots in the team, thereby enabling cooperative robots to perform tasks more efficiently.

For multirobot systems, there are two main methods of CL: centralized CL (CCL) and decentralized CL (DCL) [10], [11], [12]. In CCL, all robots share their measurements with a fusion center, where the data are processed by a central entity and all measurements can be optimally fused to jointly improve all states [13], [14]. While this centralized approach does allow accurate localization, it requires a high degree of trust in the central entity and a strong communication infrastructure due to the joint estimation of robot states and constant communication demands. Hence, a decentralized approach is needed for multirobot systems, since it can address these shortcomings by relaxing communication requirements and allocating computational costs to robots participating in the CL process [15]. In DCL, every robot processes its own measurements and exchanges information with available neighbors to determine its position [16], [17]. This method uses information from multiple sources and neither relies on a central entity nor requires a strong communication infrastructure, which makes it well suited for multirobot systems with limited communication capabilities in challenging environments. Classic Kalman filter (KF)-based CL methods are common and easy to implement in DCL [18], [19]. However, such methods can lead to inconsistent estimates because they are based on normal assumptions of conditional independence and ignore potential information interdependencies between teammates. The robots participating in the CL observe and communicate with each other, which creates a correlation between their individual estimates. Therefore, it is necessary to maintain the coupling term between any two robots in their estimation equations [20].

Ignoring these dependencies puts the reliability of localization at risk since it can lead to problems of double counting or data incest, which results in overconfidence.

Roumeliotis and Bekey [21] proposed a DCL method based on an extended KF (EKF). Their method achieves equivalent performance to the centralized method by tracking the correlation between robots based on the nondiagonal blocks of the covariance matrix, but it requires all teammates to communicate. However, for a team of N robots, all robots send motion and measurement data to a central processing unit to update their estimates, which leads to a computational complexity of $\mathcal{O}(N^2)$ and communication complexity of $\mathcal{O}(N)$ per robot. Kia et al. [22] attempts to reduce the communication during CL by introducing an additional server. In this method, the robot receives relative measurement updates from the server to opportunistically correct its state estimation. To reduce the computational complexity and large memory requirements caused by maintaining the previous inter-robot correlation, and without introducing additional infrastructure, a CL method based on covariance intersection (CI) is used to alleviate the influence of unknown cross correlation [23], [24]. This method only requires every robot to maintain its own state and covariance while ignoring the correlation between robots, where the joint covariance is calculated by a convex combination of existing uncertainties [25]. Given that the CI method uses conservative bounds to account for missing cross-covariance information and thus ensure consistency of estimation, it has often been criticized for its conservative estimates [26], [27]. Luft et al. [28] proposed a recursive DCL method, where every cross correlation is decomposed into two half-cross-correlations, and every robot recursively estimates its state and half-cross correlation with other robots, thereby maintaining approximate tracking of prior cross-covariance. Jung and Weiss [29] extended this work to the 3-D case, where decentralized cooperative state estimation was achieved by exteroceptive sensors aiding inertial navigation systems. Although their method does not guarantee strict consistency of the estimates, it shows satisfactory estimation consistency. This method also limits communication to two robots that obtain relative measurements, with lower computational and communication loads, but it can only update the state estimation of either one or both robots. Therefore, a decentralized multisource CL algorithm is needed to track the correlation between robots and fuse estimates from multiple sources.

The multisource fusion strategy of DCL aims to estimate a robot's own state by directly or indirectly fusing multisource information from sensors or other teammates. Yang et al. [30] proposed a multisensor multivehicle localization and mobility tracking framework that can fuse the information from local onboard sensors, relative measurement information from other vehicles, and observations from existing intelligent transportation system infrastructure. Although this framework can achieve multisensor multivehicle information fusion, it does not explore the impact of relative measurement correlations and faulty measurements on the localization performance of the whole system. Typically, information fusion methods employing multiple sources are based on the nominal measurement conditions of the sensors. However, in a challenging

environment, inaccurate nonlinear state space modeling and sensor failure can lead to outliers in state estimation [31], [32]. Meng and Hsu [33] proposed a resilient interactive sensor-independent-update method where multisensor integration is implemented in a state estimation domain enhanced by interactive information fusion. This method includes fault detection and exclusion (FDE) functions. However, it requires a priori information to drive the dynamic update of the model and can only be applied to a single-vehicle localization scenario. Al Hage et al. [34] proposed an information filtering method based on multisensor FDE for indoor multirobot systems, but it was designed for CCL and is not suitable for DCL due to the limited available sensor information. Wu et al. [35] applied that method to a DCL algorithm for mobile robot teams. However, any correlation between them affects localization accuracy due to the fact that the state estimation of different robots is usually considered independent. In the decentralization mechanism, there may simultaneously exist more than one type of error sources. In addition to outliers, there are also errors caused by the correlation between estimates [36]. For multirobot localization systems, underestimation or even neglect of the correlations between estimates can cause circular reasoning, which further leads to the over-convergence problem [37], [38]. These different types of errors affect the localization performance of DCL solutions, and may cause serious degradation in the robustness of the system. Therefore, we seek a decentralized multisource CL algorithm that can track inter-robot correlations and perform online validation of abnormal estimates.

Although many DCL methods have been proposed for multirobot systems, fusing multiple sources of information while considering the tracking inter-robot correlations has not been achieved. In complex environments, this degrades the accuracy and robustness of localization. To solve the above problems, this article proposes a resilient DCL (RDCL) framework that divides sensor observations into private and relative measurements. We design a tracking and updating process for cross correlation so that it is only related to relative measurements between teammates and is not affected by private measurements. The sensor measurements and state propagation system are independently integrated in an elemental filter, and measurement updates are performed in parallel. According to the output of the elemental filters, we fuse all measurement updates and information associated with the robot to be estimated to obtain more accurate state estimates. The proposed RDCL framework is decentralized and not restricted to specific models, and can perform online validation of its estimations. The main contributions of this work are as follows.

- 1) A RDCL algorithm is proposed for multisource multirobot systems. We make the measurement update processes of elemental filters independent of each other to avoid interference between measurement updates by running the private and relative measurement update procedures in parallel.
- 2) An online validation module is added to validate the estimates from different sources, thus improving the degradation of localization performance caused by

measurement uncertainty. Simulation results show that the inclusion of the validation module improves the localization accuracy of the proposed algorithm by 58%.

- 3) The overall estimate of every robot is determined by the weighted sum of multiple source estimates. An optimal information fusion algorithm is adopted to perform this calculation. This approach differs from existing DCL methods in that we can better fuse the estimates from multiple sources based on tracking correlations. Simulation results show that the proposed algorithm improves the localization performance and resilience of multirobot systems compared to existing algorithms. Experimental results using real-world dataset show that the proposed algorithm can achieve a localization accuracy with an average root mean square error (ARMSE) of 0.68 m, which is 34% better than that of the traditional DCL algorithm.

The remaining contents of this article are organized as follows. Section II presents a dynamic system model, observation model, and a preliminary and problem statement. The RDCL algorithm and its detailed implementations are presented in Section III. Then we evaluate the performance of the proposed algorithm through simulations and experiments in Section IV. Finally, conclusions are presented in Section V.

II. PRELIMINARY AND PROBLEM STATEMENT

Suppose there is a team of robots with communication, measurement, and processing capabilities. These robots are equipped with proprioceptive sensors (e.g., inertia measurement unit (IMU) or odometry) to measure physical motion and exteroceptive sensors (e.g., ultrawide band (UWB) or camera) to obtain relative measurements with teammates. In addition, some robots in the team may intermittently obtain absolute measurement information (e.g., global navigation satellite system (GNSS) or landmark).

In a team of N robots, \mathbf{x}_k^i and \mathbf{u}_k^i are the state vector and the control input of robot i at time step k , respectively, where $i \in \{1, \dots, N\}$. The physical motion of robot i can be given by the following dynamic model:

$$\hat{\mathbf{x}}_{k+1|k}^i = \mathbf{f}_k^i(\hat{\mathbf{x}}_k^i, \mathbf{u}_k^i) + \mathbf{w}_k^i. \quad (1)$$

Here \mathbf{f}_k^i is equation of the state model of robot i at time step k , and \mathbf{w}_k^i is the state noise with covariance matrix \mathbf{Q}_k^i , which is assumed to be a zero-mean white Gaussian distribution.

The observation data of robot i can be divided into two types: 1) $\hat{\mathbf{z}}_{p,k+1}^i$ denotes the private measurement at time step $k+1$, which is only related to its own state and physical motion and 2) $\hat{\mathbf{z}}_{r,k+1}^{ij}$ denotes the relative measurement at time step $k+1$, which is not only related to its own state but also to the state of another robot j , where $i, j \in \{1, \dots, N\}$.

For the private measurement $\hat{\mathbf{z}}_{p,k+1}^i$, we have

$$\hat{\mathbf{z}}_{p,k+1}^i = \mathbf{h}_{p,k+1}^i(\hat{\mathbf{x}}_{k+1|k}^i) + \mathbf{v}_{p,k+1}^i \quad (2)$$

where $\mathbf{h}_{p,k+1}^i$ is the equation of the private measurement model, which can be obtained by the inherent properties of the sensing devices and the information processing mode. $\mathbf{v}_{p,k+1}^i$ is the private measurement noise of robot i at time step $k+1$ and

is modeled as a zero-mean white Gaussian distribution with covariance matrix $\mathbf{R}_{p,k+1}^i$.

For the relative measurement $\hat{\mathbf{z}}_{r,k+1}^{ij}$, we have

$$\hat{\mathbf{z}}_{r,k+1}^{ij} = \mathbf{h}_{r,k+1}^{ij}(\hat{\mathbf{x}}_{k+1|k}^i, \hat{\mathbf{x}}_{k+1|k}^j) + \mathbf{v}_{r,k+1}^{ij} \quad (3)$$

where $\mathbf{h}_{r,k+1}^{ij}$ is the equation of the relative measurement model and is determined by the properties of the sensors, the algorithm for extracting information, and the process of transmitting information. $\hat{\mathbf{x}}_{k+1|k}^j$ is the predicted estimated state of robot j detected by robot i at time step $k+1$, and $\mathbf{v}_{r,k+1}^{ij}$ is the relative measurement noise modeled as a zero-mean white Gaussian distribution with covariance matrix $\mathbf{R}_{r,k+1}^{ij}$.

The proposed RDCL algorithm is suitable for general measurement models. However, to maintain consistency with subsequent simulations and experiments, we apply the previous general model to multirobot localization in the 2-D plane. Every robot can record the range and bearing relative to known landmarks or other robots. The dynamic system model and observation model are detailed below.

A. Dynamic System Model

The estimated state of robot i at time step k is denoted as $\hat{\mathbf{x}}_k^i = [\mathbf{p}_k^i, \theta_k^i]^T$, where $\mathbf{p}_k^i = [x_k^i, y_k^i]^T$ and θ_k^i denote the robot's position and orientation in the Cartesian coordinate system, respectively. The nonlinear discrete-time motion model of robot i is given by

$$\begin{cases} x_{k+1|k}^i = x_k^i + (V_k^i - w_{V,k}^i)\cos(\theta_k^i)\delta t \\ y_{k+1|k}^i = y_k^i + (V_k^i - w_{V,k}^i)\sin(\theta_k^i)\delta t \\ \theta_{k+1|k}^i = \theta_k^i + (\omega_k^i - w_{\omega,k}^i)\delta t \end{cases} \quad (4)$$

where V_k^i and ω_k^i are, respectively, the measured linear velocity and rotational angular velocity of robot i at time step k ; these measurements are obtained from the proprioceptive sensors, which introduce measurement noise represented by $w_{V,k}^i$ and $w_{\omega,k}^i$, respectively; δt is the discretization time.

B. Observation Model

For the private measurement of robot i , we can detect a set of previously known and distinguishable landmarks to obtain range and bearing measurements. The measurement model is given by

$$\begin{cases} d_{p,k+1}^{il} = \sqrt{(x_{k+1|k}^i - x^l)^2 + (y_{k+1|k}^i - y^l)^2} + v_{d,p,k+1}^{il} \\ \theta_{p,k+1}^{il} = \text{atan2}(y_{k+1|k}^i - y^l, x_{k+1|k}^i - x^l) - \theta_{k+1|k}^i \\ + v_{\theta,p,k+1}^{il} \end{cases} \quad (5)$$

where $d_{p,k+1}^{il}$ and $\theta_{p,k+1}^{il}$ correspond to the range and bearing measurements, respectively, of robot i to landmark l ; these measurements are obtained at time step $k+1$ by the exteroceptive sensors equipped with measurement noise $v_{d,p,k+1}^{il}$ and $v_{\theta,p,k+1}^{il}$, respectively. x^l and y^l denote the Cartesian coordinates of landmark l .

Similarly, if robot j is detected by robot i , the relative measurement model is

$$\begin{cases} d_{r,k+1}^{ij} = \sqrt{(x_{k+1|k}^i - x_{k+1|k}^j)^2 + (y_{k+1|k}^i - y_{k+1|k}^j)^2} + v_{d,r,k+1}^{ij} \\ \theta_{r,k+1}^{ij} = \text{atan2}(y_{k+1|k}^i - y_{k+1|k}^j, x_{k+1|k}^i - x_{k+1|k}^j) - \theta_{k+1|k}^i + v_{\theta,r,k+1}^{ij} \end{cases} \quad (6)$$

where $d_{r,k+1}^{ij}$ and $\theta_{r,k+1}^{ij}$ denote the measured relative range and bearing between robots i and j at time $k+1$, respectively; these measurements are obtained by exteroceptive sensors with measurement noise $v_{d,r,k+1}^{ij}$ and $v_{\theta,r,k+1}^{ij}$, respectively; x_{k+1}^j and y_{k+1}^j represent the Cartesian coordinates of robot j .

C. Problem Statement

In DCL, robot i provides a state estimate $\hat{\mathbf{x}}_k^i$ and corresponding covariance matrix $\hat{\mathbf{P}}_k^i$ at time step k . According to [28], to track inter-robot dependencies, the cross correlation $\{\hat{\mathbf{P}}_k^{ij}\}_{1 \leq i, j \leq N}^{j \neq i}$ is decomposed into two half-cross-covariances, which can be recursively estimated.

The robots might be uncorrelated at the beginning of their mission, which means $\hat{\mathbf{P}}_k^{ij} = 0$ for all $i \neq j$. If robot j is detected by robot i at time step k , we generally assume that $\hat{\mathbf{P}}_k^{ij} \neq 0$, and decompose $\hat{\mathbf{P}}_k^{ij}$ as follows:

$$\hat{\mathbf{P}}_k^{ij} = \sigma_k^{ij} (\sigma_k^{ji})^T \quad (7)$$

where the recursive estimates of the half-cross-correlations σ_k^{ij} and σ_k^{ji} are performed locally by robots i and robot j , respectively.

However, the communication and relative measurement update of the traditional DCL method is limited to two robots [28], [29], and no specific measurement update strategy is given when multiple targets are detected. In addition, the tracking and updating of cross-covariance is related to the private measurement and the relative measurement, which easily leads to errors in the private measurement update affecting the relative measurement update. In this article, the proposed RDCL algorithm allows for simultaneously detecting multiple targets and tracking inter-robot dependencies, which estimates state by fusing information from multiple sources based on an optimal fusion criterion. Meanwhile, the proposed algorithm supports general measurement models and online validation of multiple sensors, which ensures accurate and resilient localization.

III. RDCL ALGORITHM

Here we present the proposed RDCL algorithm in detail. Fig. 1 shows the framework. The input of robot i is an estimated state $\hat{\mathbf{x}}_k^i$ and corresponding covariance matrix $\hat{\mathbf{P}}_k^i$ at time step k . Every available sensor measurement of the robot is integrated with a state propagated module in an elemental filter. There is no correlation between different sensor measurement. For the elemental filter, the state propagation is performed with the same proprioceptive sensor. Then, the elemental filters perform private measurement and

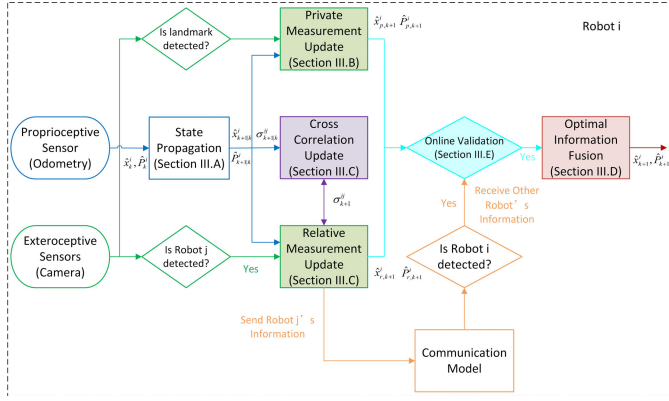


Fig. 1. RDCL framework for multirobot systems. The filled blocks are the works in this study.

relative measurement updates in parallel; note that the relative measurement update needs to track the cross-covariance. It is assumed that a relative measurement occurred between robots i and j ; their individual state estimations and the relative measurement information need to be shared and transmitted through the communication module. The overall estimation $\hat{\mathbf{x}}_{k+1}^i$ and corresponding covariance matrix $\hat{\mathbf{P}}_{k+1}^i$ are determined by the weighted sum of estimates from elemental filters and information received from other robots. To ensure the accuracy and reliability of localization, a fault detection method is added to the elemental filter for online validation.

A. State Propagation

Assuming that the movements of all teammates are independent, robot i estimates its state through its own proprioception sensor. It has a control input \mathbf{u}_k^i of odometry measurement or velocity command.

To track and maintain dependencies during state propagation, according to [21], robot i can update the half-cross correlation with robot j by

$$\sigma_{k+1|k}^{ij} = \mathbf{F}_k^i \sigma_k^{ij}. \quad (8)$$

The state propagation of robot i is shown in Algorithm 1.

B. Private Measurement Update

Robot i performs a private measurement update through the elemental filter to obtain the local estimation $\hat{\mathbf{x}}_{p,k+1}^i$ and corresponding covariance matrix $\hat{\mathbf{P}}_{p,k+1}^i$ at time step $k+1$. In our article, robots can detect a set of known and distinguishable landmarks to obtain range and bearing measurements. We denote L_{k+1}^i as the set of landmarks detected by robot i at time step $k+1$.

According to (2), if landmark l is detected by robot i , the private measurement model is $\mathbf{h}_{p,k+1}^{il}$ and the augmented private measurement is

$$\mathbf{z}_{p,k+1}^{iL_{k+1}^i} = \text{col}\{\mathbf{z}_{p,k+1}^{il}\}_{l \in L_{k+1}^i}. \quad (9)$$

The corresponding augmented private measurement noise covariance matrix is

$$\mathbf{R}_{p,k+1}^{iL_{k+1}^i} = \text{diag}\{\mathbf{R}_{p,k+1}^{il}\}_{l \in L_{k+1}^i}. \quad (10)$$

Algorithm 1 State Propagation for Robot i

Input: $\hat{\mathbf{x}}_k^i, \hat{\mathbf{P}}_k^i, \{\sigma_k^{ij}\}_{1 \leq j \leq N, j \neq i}^i, \mathbf{u}_k^i, \mathbf{Q}_k^i$

Output: $\hat{\mathbf{x}}_{k+1|k}^i, \hat{\mathbf{P}}_{k+1|k}^i, \{\sigma_{k+1|k}^{ij}\}_{1 \leq j \leq N, j \neq i}^i$

1. Predicted state vector:

$$\hat{\mathbf{x}}_{k+1|k}^i = \mathbf{f}_k^i(\hat{\mathbf{x}}_k^i, \mathbf{u}_k^i)$$

2. State Jacobi matrix:

$$\mathbf{F}_k^i = \frac{\partial \mathbf{f}_k^i(\mathbf{x}_k^i, \mathbf{u}_k^i)}{\partial \mathbf{x}_k^i}(\hat{\mathbf{x}}_k^i, \mathbf{u}_k^i)$$

3. State noise Jacobi matrix:

$$\mathbf{G}_k^i = \frac{\partial \mathbf{f}_k^i(\mathbf{x}_k^i, \mathbf{u}_k^i)}{\partial \mathbf{w}_k^i}(\hat{\mathbf{x}}_k^i, \mathbf{u}_k^i)$$

4. Prediction covariance matrix:

$$\hat{\mathbf{P}}_{k+1|k}^i = \mathbf{F}_k^i \hat{\mathbf{P}}_k^i (\mathbf{F}_k^i)^T + \mathbf{G}_k^i \mathbf{Q}_k^i (\mathbf{G}_k^i)^T$$

5. Predicted half-cross-correlations:

$$\text{for } 1 \leq j \leq N, j \neq i \text{ do} \\ \sigma_{k+1|k}^{ij} = \mathbf{F}_k^i \sigma_k^{ij} \\ \text{end}$$

Algorithm 2 Private Measurement Update for Robot i

Input: $\hat{\mathbf{x}}_{k+1|k}^i, \hat{\mathbf{P}}_{k+1|k}^i, \{\mathbf{z}_{p,k+1}^{il}, \mathbf{R}_{p,k+1}^{il}, \mathbf{x}^l\}_{l \in L_{k+1}^i}^i$

Output: $\hat{\mathbf{x}}_{p,k+1}^i, \hat{\mathbf{P}}_{p,k+1}^i$

1. Predicted augmented private measurement:

$$\hat{\mathbf{z}}_{p,k+1}^{iL_{k+1}^i} = \text{col}\{\hat{\mathbf{z}}_{p,k+1}^{il}\}_{l \in L_{k+1}^i}, \text{ where } \hat{\mathbf{z}}_{p,k+1}^{il} =$$

$$\mathbf{h}_{p,k+1}^{il}(\hat{\mathbf{x}}_{k+1|k}^i, \mathbf{x}^l)$$

2. Augmented private measurement Jacobi matrix:

$$\mathbf{H}_{p,k+1}^{iL_{k+1}^i} = \text{row}\{\mathbf{H}_{p,k+1}^{il}\}_{l \in L_{k+1}^i}, \text{ where } \mathbf{H}_{p,k+1}^{il} =$$

$$\frac{\partial \mathbf{h}_{p,k+1}^{il}(\hat{\mathbf{x}}_{k+1|k}^i, \mathbf{x}^l)}{\partial \mathbf{x}_{k+1}^i}(\hat{\mathbf{x}}_{k+1|k}^i)$$

3. Kalman gain of augmented private measurement:

$$\mathbf{K}_{p,k+1}^{iL_{k+1}^i} = \hat{\mathbf{P}}_{k+1|k}^i (\mathbf{H}_{p,k+1}^{iL_{k+1}^i})^T [\mathbf{H}_{p,k+1}^{iL_{k+1}^i} \hat{\mathbf{P}}_{k+1|k}^i (\mathbf{H}_{p,k+1}^{iL_{k+1}^i})^T + \mathbf{R}_{p,k+1}^{iL_{k+1}^i}]^{-1}$$

4. State estimate:

$$\hat{\mathbf{x}}_{p,k+1}^i = \hat{\mathbf{x}}_{k+1|k}^i + \mathbf{K}_{p,k+1}^{iL_{k+1}^i} [\mathbf{z}_{p,k+1}^{iL_{k+1}^i} - \hat{\mathbf{z}}_{p,k+1}^{iL_{k+1}^i}]$$

5. Estimation covariance matrix:

$$\hat{\mathbf{P}}_{p,k+1}^i = [\mathbf{I} - \mathbf{K}_{p,k+1}^{iL_{k+1}^i} \mathbf{H}_{p,k+1}^{iL_{k+1}^i}] \hat{\mathbf{P}}_{k+1|k}^i$$

Due to the occlusion of known landmarks caused by the surrounding environment, any robot may occasionally access private measurements. Different from the traditional DCL method, the proposed algorithm processes private and relative measurements in parallel by forming multiple elemental filters without updating the private cross correlation covariance. This prevents the private measurement update from influencing the relative measurement update. The private measurement update is shown in Algorithm 2.

C. Relative Measurement Update

The relative measurement update requires estimates from one or more other robots in addition to the robot's own state estimates. When robot j is successfully detected by robot i , it sends its own state, corresponding covariance, and half-cross correlation to robot i . This communication only takes

place between the robots involved in the relative measurement update. According to (3), the relative measurement model is $\mathbf{h}_{r,k+1}^{ij}$.

Robot i can obtain the local estimation $\hat{\mathbf{x}}_{r,k+1}^i$ and corresponding covariance matrix $\hat{\mathbf{P}}_{r,k+1}^i$ at time step $k+1$ through the local elemental filter. J_{k+1}^i is the set of robots detected by robot i at time step $k+1$. The information received from robot set J_{k+1}^i is given by

$$\left\{ \hat{\mathbf{x}}_{k+1|k}^j, \hat{\mathbf{P}}_{k+1|k}^j, \sigma_{k+1|k}^{js} \right\}_{s,j \in J_{k+1}^i}^{s \neq j}. \quad (11)$$

The augmented state estimation and the corresponding augmented estimation covariance matrix of robots in J_{k+1}^i are

$$\hat{\mathbf{x}}_{k+1|k}^{J_{k+1}^i} = \text{col} \left\{ \hat{\mathbf{x}}_{k+1|k}^j \right\}_{j \in J_{k+1}^i} \quad (12)$$

$$\hat{\mathbf{P}}_{k+1|k}^{J_{k+1}^i} = \text{block} \left\{ \hat{\mathbf{P}}_{k+1|k}^j, \hat{\mathbf{P}}_{k+1|k}^{js} \right\}_{s,j \in J_{k+1}^i}^{s \neq j} \quad (13)$$

where

$$\hat{\mathbf{P}}_{k+1|k}^{js} = \sigma_{k+1|k}^{js} \left(\sigma_{k+1|k}^{sj} \right)^T. \quad (14)$$

The augmented relative measurement and the corresponding augmented relative measurement noise covariance matrix are

$$\mathbf{z}_{r,k+1}^{J_{k+1}^i} = \text{col} \left\{ \mathbf{z}_{r,k+1}^{ij} \right\}_{j \in J_{k+1}^i} \quad (15)$$

$$\mathbf{R}_{r,k+1}^{J_{k+1}^i} = \text{diag} \left\{ \mathbf{R}_{r,k+1}^{ij} \right\}_{j \in J_{k+1}^i}. \quad (16)$$

The input of the relative measurement updates of the proposed algorithm do not involve private measurement updates, i.e., the private measurement updates do not affect the relative measurement updates. Every robot is allowed to acquire relative measurements from multiple robots, and the communication only occurs between robots involved in relative measurement updates. Moreover, the dependencies of the robots involved in relative measurement updates can be reproduced by sharing the cross correlation. The estimation from the relative measurement update only depends on the current state of the robots cooperating. Algorithm 3 details the relative measurement update.

D. Global Fusion for Multisource Information

The proposed algorithm has a two-layer structure: it consists of elemental filters and a global filter. In the elemental filters, observable sensor measurements are integrated with the propagated system to update the private and relative measurements and to obtain a set of estimates of the robot's own state. Meanwhile, if another robot observes the robot to be estimated, it can generate the state of that robot using its own set of elemental filters; then, it can share its estimation results according to Algorithm 3. The local estimates related to a robot, including the private measurement update, relative measurement update, and information received from other robots, are input into a global filter based on their weights. This allows us to obtain a more accurate global estimate for the robot. The same procedure applies to all robots, and thus we have a decentralized framework.

Algorithm 3 Relative Measurement Update for Robot i

-
- Input:** $\hat{\mathbf{x}}_{k+1|k}^i, \hat{\mathbf{P}}_{k+1|k}^i, \left\{ \sigma_{k+1|k}^{ij} \right\}_{j \in J_{k+1}^i}^{j \neq i}, \left\{ \hat{\mathbf{x}}_{k+1|k}^j, \hat{\mathbf{P}}_{k+1|k}^j, \sigma_{k+1|k}^{js} \right\}_{s,j \in J_{k+1}^i}^{s \neq j}, \left\{ \mathbf{z}_{r,k+1}^{ij}, \mathbf{R}_{r,k+1}^{ij} \right\}_{j \in J_{k+1}^i}$
- Output:** $\hat{\mathbf{x}}_{r,k+1}^i, \hat{\mathbf{P}}_{r,k+1}^i, \left\{ \sigma_{k+1}^{ij} \right\}_{j \in J_{k+1}^i}^{j \neq i}$
1. Reproduced cross correlation:

$$\hat{\mathbf{P}}_{r,k+1|k}^{J_{k+1}^i} = \text{row} \left\{ \hat{\mathbf{P}}_{r,k+1|k}^{ij} \right\}_{j \in J_{k+1}^i}^{j \neq i}, \text{ where } \hat{\mathbf{P}}_{r,k+1|k}^{ij} = \sigma_{k+1|k}^{ij} \left(\sigma_{k+1|k}^{ji} \right)^T$$
 2. Augmented estimation covariance matrix:

$$\hat{\mathbf{P}}_{r,k+1|k}^{(a)} = \begin{bmatrix} \hat{\mathbf{P}}_{k+1|k}^i & \hat{\mathbf{P}}_{r,k+1|k}^{J_{k+1}^i} \\ \left(\hat{\mathbf{P}}_{r,k+1|k}^{J_{k+1}^i} \right)^T & \hat{\mathbf{P}}_{r,k+1|k}^{J_{k+1}^i} \end{bmatrix}$$
 3. Predicted augmented relative measurement:

$$\hat{\mathbf{z}}_{r,k+1}^{J_{k+1}^i} = \text{col} \left\{ \mathbf{z}_{r,k+1}^{ij} \right\}_{j \in J_{k+1}^i}, \text{ where } \hat{\mathbf{z}}_{r,k+1}^{ij} = \mathbf{h}_{r,k+1}^{ij} \left(\hat{\mathbf{x}}_{k+1|k}^i, \hat{\mathbf{x}}_{k+1|k}^j \right)$$
 4. Augmented measurement Jacobi matrix:

$$\mathbf{H}_{r,k+1}^{J_{k+1}^i} = \text{block} \left\{ \mathbf{H}_{r,k+1}^i, \mathbf{H}_{r,k+1}^j, \mathbf{H}_{r,k+1}^s \right\}_{s,j \in J_{k+1}^i}^{s \neq j},$$

where $\mathbf{H}_{r,k+1}^i = \frac{\partial \mathbf{h}_{r,k+1}^{ij}(\mathbf{x}_{k+1}^i, \mathbf{x}_{k+1}^j)}{\partial \mathbf{x}_{k+1}^i} (\hat{\mathbf{x}}_{k+1|k}^i, \hat{\mathbf{x}}_{k+1|k}^j)$, $\mathbf{H}_{r,k+1}^j = \frac{\partial \mathbf{h}_{r,k+1}^{ij}(\mathbf{x}_{k+1}^i, \mathbf{x}_{k+1}^j)}{\partial \mathbf{x}_{k+1}^j} (\hat{\mathbf{x}}_{k+1|k}^i, \hat{\mathbf{x}}_{k+1|k}^j)$ and $\mathbf{H}_{r,k+1}^s = \mathbf{0}$
 5. Kalman gain of augmented relative measurement:

$$\mathbf{K}_{r,k+1}^{J_{k+1}^i} = \hat{\mathbf{P}}_{r,k+1|k}^{(a)} \left(\mathbf{H}_{r,k+1}^{J_{k+1}^i} \right)^T \left[\mathbf{H}_{r,k+1}^{J_{k+1}^i} \hat{\mathbf{P}}_{r,k+1|k}^{(a)} \left(\mathbf{H}_{r,k+1}^{J_{k+1}^i} \right)^T + \mathbf{R}_{r,k+1}^{J_{k+1}^i} \right]^{-1}$$
 6. State estimate:

$$\begin{bmatrix} \hat{\mathbf{x}}_{r,k+1}^i \\ \hat{\mathbf{x}}_{r,k+1}^{J_{k+1}^i} \end{bmatrix} = \begin{bmatrix} \hat{\mathbf{x}}_{k+1|k}^i \\ \hat{\mathbf{x}}_{k+1|k}^{J_{k+1}^i} \end{bmatrix} + \mathbf{K}_{r,k+1}^{J_{k+1}^i} \left[\mathbf{z}_{r,k+1}^{J_{k+1}^i} - \hat{\mathbf{z}}_{r,k+1}^{J_{k+1}^i} \right]$$
 7. Estimation covariance matrix:

$$\begin{bmatrix} \hat{\mathbf{P}}_{r,k+1}^i & \hat{\mathbf{P}}_{r,k+1}^{J_{k+1}^i} \\ \left(\hat{\mathbf{P}}_{r,k+1}^{J_{k+1}^i} \right)^T & \hat{\mathbf{P}}_{r,k+1}^{J_{k+1}^i} \end{bmatrix} = \left[\mathbf{I} - \mathbf{K}_{r,k+1}^{J_{k+1}^i} \mathbf{H}_{r,k+1}^{J_{k+1}^i} \right] \hat{\mathbf{P}}_{r,k+1|k}^{(a)}$$
 8. Estimated half cross-correlations with robot j :

$$\left\{ \sigma_{k+1}^{ij} = \hat{\mathbf{P}}_{r,k+1}^{ij} \right\}_{j \in J_{k+1}^i}^{j \neq i}$$
 9. Send to robot j :

$$\left\{ \hat{\mathbf{x}}_{i,k+1}^j, \hat{\mathbf{P}}_{i,k+1}^j, \sigma_{k+1}^{ji} = \mathbf{I} \right\}_{j \in J_{k+1}^i}$$
 10. Estimated half cross-correlations between robot i and nonparticipating robot n :
for $n = 1 : N, n \notin \{i, J_{k+1}^i\}$ **do**

$$\sigma_{k+1}^{in} = \hat{\mathbf{P}}_{r,k+1}^i \left(\hat{\mathbf{P}}_{k+1|k}^n \right)^{-1} \sigma_{k+1|k}^{in}$$

end
 11. **if** robot j detects robot i **then**
Receive information from robot i : $\hat{\mathbf{x}}_{k+1|k}^i, \hat{\mathbf{P}}_{k+1|k}^i, \sigma_{k+1|k}^{ij}$
Send information to robot i : $\hat{\mathbf{x}}_{j,k+1}^i, \hat{\mathbf{P}}_{j,k+1}^i, \sigma_{k+1}^{ij} = \mathbf{I}$
-

The goal of the global filter is to fuse the outputs of the elemental filters to obtain the optimal estimate of robot i . We assume that the measurement of the sensor used in this article is Gaussian, and thus the result of the elemental filter is Gaussian. Then, the global optimal state estimation can be expressed as a linear combination of local estimates.

In other words, the problem becomes an information fusion problem similar to that of a single robot with multisource information in a linear Gaussian system. The global estimation $\hat{\mathbf{x}}_{k+1}^i$ and the corresponding covariance $\hat{\mathbf{P}}_{k+1}^i$ can be expressed as

$$\hat{\mathbf{x}}_{k+1}^i = \mathbf{A}_{p,k+1}^i \hat{\mathbf{x}}_{p,k+1}^i + \mathbf{A}_{r,k+1}^i \hat{\mathbf{x}}_{r,k+1}^i + \sum_{j=1}^{T_{k+1}^i} \mathbf{A}_{j,k+1}^i \hat{\mathbf{x}}_{j,k+1}^i \quad (17)$$

$$\begin{aligned} \hat{\mathbf{P}}_{k+1}^i &= \mathbf{A}_{p,k+1}^i \hat{\mathbf{P}}_{p,k+1}^i (\mathbf{A}_{p,k+1}^i)^T \\ &+ \mathbf{A}_{r,k+1}^i \hat{\mathbf{P}}_{r,k+1}^i (\mathbf{A}_{r,k+1}^i)^T \\ &+ \sum_{j=1}^{T_{k+1}^i} \mathbf{A}_{j,k+1}^i \hat{\mathbf{P}}_{j,k+1}^i (\mathbf{A}_{j,k+1}^i)^T \end{aligned} \quad (18)$$

where $\mathbf{A}_{p,k+1}^i$, $\mathbf{A}_{r,k+1}^i$, and $\mathbf{A}_{j,k+1}^i$ are the weights of the linear combination to be determined; $\mathbf{A}_{p,k+1}^i$ is the weight of the private measurement update; $\mathbf{A}_{r,k+1}^i$ is the weight of the relative measurement update; and $\mathbf{A}_{j,k+1}^i$ is the weight of the estimate received from other robots. T_{k+1}^i is the number of estimates of robot i received from other robots at time step $k+1$.

Assuming that the global estimator is unbiased, we have the following constraint on $\mathbf{A}_{p,k+1}^i$, $\mathbf{A}_{r,k+1}^i$, and $\mathbf{A}_{j,k+1}^i$:

$$\mathbf{A}_{p,k+1}^i + \mathbf{A}_{r,k+1}^i + \sum_{j=1}^{T_{k+1}^i} \mathbf{A}_{j,k+1}^i = \mathbf{I}. \quad (19)$$

According to the above Gaussian assumption, the weighted parameters would be optimally determined based on a minimum variance (maximum likelihood) criterion. Therefore, the global fusion becomes an optimization problem

$$\begin{aligned} &\min_{\mathbf{A}_{1,k+1}^i, \dots, \mathbf{A}_{T_{k+1}^i,k+1}^i, \mathbf{A}_{p,k+1}^i, \mathbf{A}_{r,k+1}^i} \text{tr}(\hat{\mathbf{P}}_{k+1}^i) \\ &= \text{tr} \left(\mathbf{A}_{p,k+1}^i \hat{\mathbf{P}}_{p,k+1}^i (\mathbf{A}_{p,k+1}^i)^T + \mathbf{A}_{r,k+1}^i \hat{\mathbf{P}}_{r,k+1}^i (\mathbf{A}_{r,k+1}^i)^T \right. \\ &\quad \left. + \sum_{j=1}^{T_{k+1}^i} \mathbf{A}_{j,k+1}^i \hat{\mathbf{P}}_{j,k+1}^i (\mathbf{A}_{j,k+1}^i)^T \right) \\ &\text{s.t. } \mathbf{A}_{p,k+1}^i + \mathbf{A}_{r,k+1}^i + \sum_{j=1}^{T_{k+1}^i} \mathbf{A}_{j,k+1}^i = \mathbf{I} \end{aligned} \quad (20)$$

where $\mathbf{A}_{p,k+1}^i$, $\mathbf{A}_{r,k+1}^i$, and $\mathbf{A}_{j,k+1}^i$ are positive semidefinite matrices.

The convex optimization problem can be solved by the Lagrange multiplier method. The objective function is constructed as follows:

$$\begin{aligned} L(\mathbf{A}, \lambda) &= \text{tr} \left(\mathbf{A}_{p,k+1}^i \hat{\mathbf{P}}_{p,k+1}^i (\mathbf{A}_{p,k+1}^i)^T \right. \\ &\quad \left. + \mathbf{A}_{r,k+1}^i \hat{\mathbf{P}}_{r,k+1}^i (\mathbf{A}_{r,k+1}^i)^T \right. \end{aligned}$$

Algorithm 4 Global Fusion for Robot i

Input: $\{\hat{\mathbf{x}}_{p,k+1}^i, \hat{\mathbf{P}}_{p,k+1}^i\}, \{\hat{\mathbf{x}}_{r,k+1}^i, \hat{\mathbf{P}}_{r,k+1}^i\}, \{\hat{\mathbf{x}}_{j,k+1}^i, \hat{\mathbf{P}}_{j,k+1}^i\}_{j \in T_{k+1}^i}$

Output: $\hat{\mathbf{x}}_{k+1}^i, \hat{\mathbf{P}}_{k+1}^i$

1. Optimal weights for the linear combination:

$$\mathbf{A}_{p,k+1}^i = (\hat{\mathbf{P}}_{p,k+1}^i)^{-1} \left(\sum_{j=1}^{T_{k+1}^i} (\hat{\mathbf{P}}_{j,k+1}^i)^{-1} + (\hat{\mathbf{P}}_{p,k+1}^i)^{-1} + (\hat{\mathbf{P}}_{r,k+1}^i)^{-1} \right)^{-1}$$

$$\mathbf{A}_{r,k+1}^i = (\hat{\mathbf{P}}_{r,k+1}^i)^{-1} \left(\sum_{j=1}^{T_{k+1}^i} (\hat{\mathbf{P}}_{j,k+1}^i)^{-1} + (\hat{\mathbf{P}}_{p,k+1}^i)^{-1} + (\hat{\mathbf{P}}_{r,k+1}^i)^{-1} \right)^{-1}$$

$$\mathbf{A}_{j,k+1}^i = (\hat{\mathbf{P}}_{j,k+1}^i)^{-1} \left(\sum_{j=1}^{T_{k+1}^i} (\hat{\mathbf{P}}_{j,k+1}^i)^{-1} + (\hat{\mathbf{P}}_{p,k+1}^i)^{-1} + (\hat{\mathbf{P}}_{r,k+1}^i)^{-1} \right)^{-1}$$

2. Global state estimate:

$$\hat{\mathbf{x}}_{k+1}^i = \mathbf{A}_{p,k+1}^i \hat{\mathbf{x}}_{p,k+1}^i + \mathbf{A}_{r,k+1}^i \hat{\mathbf{x}}_{r,k+1}^i$$

$$+ \sum_{j=1}^{T_{k+1}^i} \mathbf{A}_{j,k+1}^i \hat{\mathbf{x}}_{j,k+1}^i$$

$$\begin{aligned} \hat{\mathbf{P}}_{k+1}^i &= \mathbf{A}_{p,k+1}^i \hat{\mathbf{P}}_{p,k+1}^i (\mathbf{A}_{p,k+1}^i)^T \\ &+ \mathbf{A}_{r,k+1}^i \hat{\mathbf{P}}_{r,k+1}^i (\mathbf{A}_{r,k+1}^i)^T \\ &+ \sum_{j=1}^{T_{k+1}^i} \mathbf{A}_{j,k+1}^i \hat{\mathbf{P}}_{j,k+1}^i (\mathbf{A}_{j,k+1}^i)^T \end{aligned}$$

$$\begin{aligned} &\cdot \sum_{j=1}^{T_{k+1}^i} \mathbf{A}_{j,k+1}^i \hat{\mathbf{P}}_{j,k+1}^i (\mathbf{A}_{j,k+1}^i)^T \Big) \\ &+ \lambda^T \left(\mathbf{A}_{p,k+1}^i + \mathbf{A}_{r,k+1}^i + \sum_{j=1}^{T_{k+1}^i} \mathbf{A}_{j,k+1}^i - \mathbf{I} \right) \lambda \end{aligned} \quad (21)$$

where λ is the Lagrange multiplier. The optimal weights of the global filter are shown in Algorithm 4.

E. Reliability Check

In this article, the normalized solution separation (NSS) method is introduced into the DCL algorithm to evaluate the outputs of the elemental filters online. The test statistic of NSS is consistent estimators of error measurements, which performance is independent of the monitored output.

The state estimates and corresponding covariances of the global estimate and local estimate are $\hat{\mathbf{x}}_{k+1}^i$, $\hat{\mathbf{P}}_{k+1}^i$, $\hat{\mathbf{x}}_{m,k+1}^i$, and $\hat{\mathbf{P}}_{m,k+1}^i$, respectively, where m indicates that the state estimate and the corresponding covariance are from the private

measurement update, relative measurement update, or other robots. The threshold for fault detection is TD.

The solution separation vector between the global estimate and the m th estimate is defined as

$$\beta_{m,k+1}^i = \hat{\mathbf{x}}_{k+1}^i - \hat{\mathbf{x}}_{m,k+1}^i. \quad (22)$$

The eigenvalue decomposition of the covariance of solution separation is

$$\begin{aligned} \mathbf{B}_{m,k+1}^i &= \hat{\mathbf{P}}_{k+1}^i - \hat{\mathbf{P}}_{m,k+1}^i \\ &= \mathbf{V}_{m,k+1}^i \mathbf{S}_{m,k+1}^i (\mathbf{V}_{m,k+1}^i)^T. \end{aligned} \quad (23)$$

The fault detection test statistic is

$$\lambda_{m,k+1}^i = (\mathbf{y}_{m,k+1}^i)^T \mathbf{y}_{m,k+1}^i \quad (24)$$

where

$$\mathbf{y}_{m,k+1}^i = (\mathbf{S}_{m,k+1}^i)^{-1/2} (\mathbf{V}_{m,k+1}^i)^T \beta_{m,k+1}^i. \quad (25)$$

A fault is declared if the following occurs:

$$(\lambda_{m,k+1}^i)^{-1/2} \geq \text{TD} \quad \text{for any } m. \quad (26)$$

It means that the state of the local estimate deviates significantly from the global estimate. Therefore, the local estimate with fault is discarded.

IV. SIMULATION AND EXPERIMENTAL VERIFICATION

A. Simulation

In this section, the performance of the proposed RDCL algorithm is validated via a series of simulations. A group of $N = 6$ homogeneous robots randomly move in a 2-D environment according to the motion model in (4). The true linear velocity of every robot is $V_k = 0.5$ m/s, while the true angular velocity of every robot is randomly selected from the uniform distribution of $[-(\pi/6), (\pi/6)]$ rad/s. The discretization time is set as $\delta t = 0.5$ s. A wheel encoder is selected as the proprioceptive sensor; it is used to measure the linear and rotational angular velocities and has the same measurement accuracy for every robot. The linear velocity noise and rotational angular velocity noise are assumed to be white Gaussian, with standard deviation of $\sigma_{V_k} = 0.02$ m and $\sigma_{\omega_k} = 1^\circ$, respectively. The six robots move from different starting positions and follow the true trajectories shown in Fig. 2. The total simulation time is $t_{\text{total}} = 400$ s.

To fully validate the proposed algorithm, we assume that there are no private measurements in the simulation and that relative measurements are generated randomly over time. The team members can achieve localization without additional external facilities; thus, they rely only on the multirobot system. In Section IV-B, every robot can obtain private measurements by detecting a set of known landmarks. The relative measurement model is given by (6). The standard deviation of relative range measurement noise is $\sigma_{d_k} = 2$ m, and the standard deviation of relative bearing measurement noise is $\sigma_{\theta_k} = 3^\circ$. The initial state \mathbf{x}_0 is set to be initial true state, and the associated initial covariance is $\sigma_{\theta_k} = 0.01 * \mathbf{I}_{3 \times 3}$. The simulation parameters are summarized in Table I.

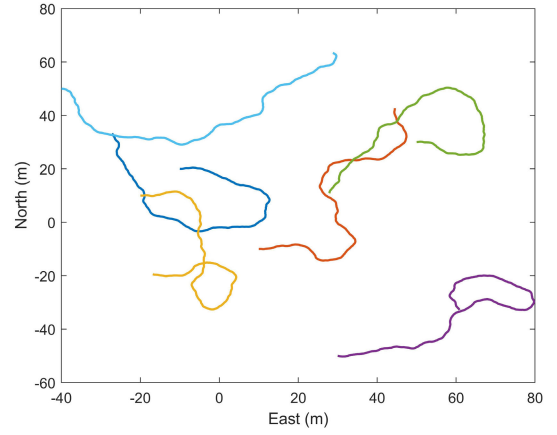


Fig. 2. True trajectories of a team of six robots.

TABLE I
SIMULATION PARAMETERS

Parameter	Symbol	Value
Discrete time step	δt	0.5 s
Duration of simulation	t_{total}	400 s
Standard deviation of linear velocity	σ_{V_k}	0.02 m/s
Standard deviation of rotational angular velocity	σ_{ω_k}	1°
Initial covariance of state	\mathbf{P}_0	$0.01 * \mathbf{I}_{3 \times 3}$
Standard deviation of relative range measurement noise	σ_{d_k}	2 m
Standard deviation of relative bearing measurement noise	σ_{θ_k}	3°

We compare the following CL algorithms over 100 Monte Carlo runs in the simulation. Detailed descriptions of the four algorithms are provided below.

- 1) *CCL* [21]: CL algorithm using the centralized joint EKF.
- 2) *DCL* [28]: DCL algorithm for multirobot systems with asynchronous pairwise communication.
- 3) *OIF* [30]: Optimal information localization algorithm for multisensor multivehicle systems.
- 4) *RDCL*: The proposed RDCL algorithm.

Note that the CCL algorithm is used as a benchmark. All algorithms are executed on laptop running on Windows 10 with an Intel Core i7-9750H CPU at 2.60 GHz.

Fig. 3 shows the root mean square error (RMSE) of position of the proposed algorithm compared to the three other algorithms. The results illustrate that the RMSE of position of the proposed RDCL algorithm is smaller than those of the existing DCL and OIF algorithms yet similar to that of the CCL algorithm. Table II lists the ARMSE of position and the average normalized estimation error squared (ANEES) of the four algorithms. In theory, the NEES value should not exceed the state dimension (i.e., $\text{NEES} \leq 3$) if the state estimate is consistent. We can see from Table II that the ANEES of the RDCL and CCL algorithms are within 3. However, the ANEES of the OIF algorithm is several orders of magnitude worse than the three other algorithms. For the OIF algorithm, the cross-covariances are usually unknown. It neglects all correlations, resulting in an underestimation of the uncertainty between state estimates. By analyzing the simulation results, we found that the covariance after fusion differs significantly from the

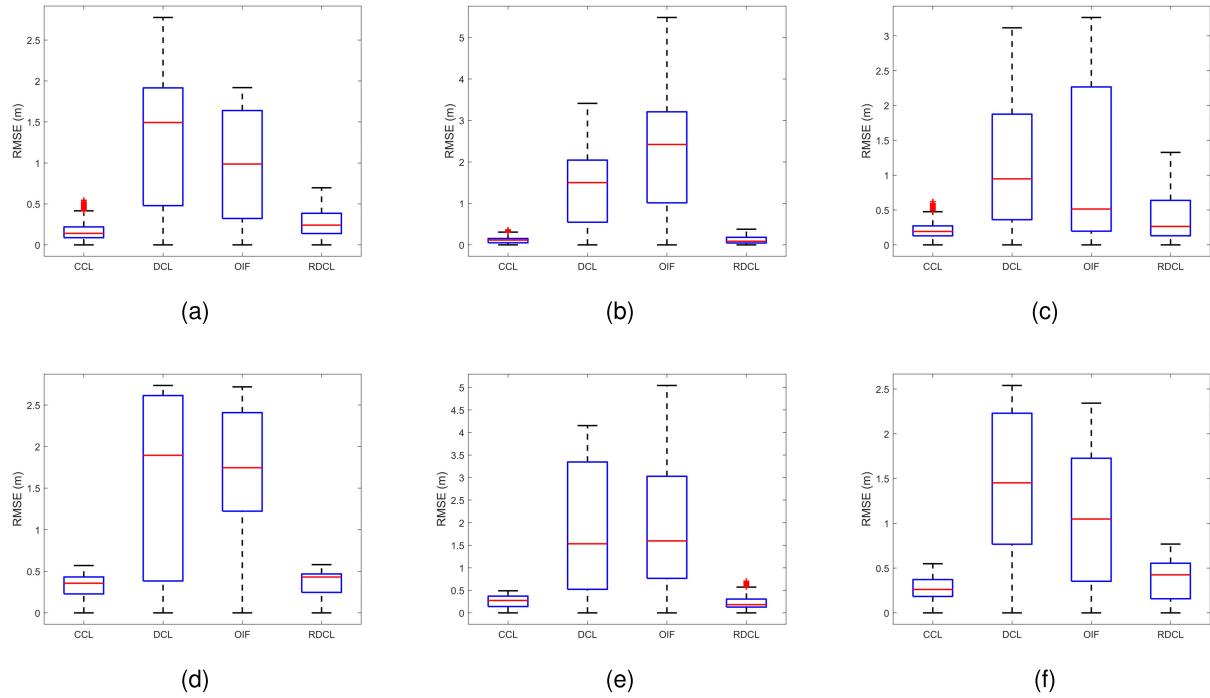


Fig. 3. RMSE of position of all of the algorithms for six robots. (a) Robot 1. (b) Robot 2. (c) Robot 3. (d) Robot 4. (e) Robot 5. (f) Robot 6.

TABLE II
ARMSE AND ANEES OF POSITIONS OF ALL OF THE ALGORITHMS FOR SIX ROBOTS

Algorithm	Metrics	Robot 1	Robot 2	Robot 3	Robot 4	Robot 5	Robot 6
CCL	ARMSE (m)	0.17	0.12	0.22	0.33	0.26	0.28
	ANEES	0.79	0.90	0.90	2.31	2.19	2.79
DCL	ARMSE (m)	1.31	1.48	1.13	1.61	1.89	1.43
	ANEES	0.77	0.89	0.27	0.74	0.35	0.49
OIF	ARMSE (m)	0.94	2.35	1.17	1.66	1.97	1.05
	ANEES	7371.61	4831.57	561.83	4348.40	10710.20	5804.86
RDCL	ARMSE (m)	0.27	0.12	0.42	0.36	0.24	0.39
	ANEES	0.72	0.53	1.93	2.04	1.32	2.56

three other algorithms (not within an order of magnitude). Thus, the proposed RDCL algorithm has better CL accuracy as well as good estimation consistency.

Fig. 4 shows the impact of the number of robots cooperating on localization performance. We calculate the RMSE of position for different numbers of cooperating robots. It can be seen that the localization performance of the proposed RDCL algorithm is closest to the CCL algorithm when the number of cooperating robots is small. As the number of cooperating robots increases, the position error of all of the algorithms decreases; the localization performance of the proposed algorithm is still closest to that of the CCL algorithm. However, when the number of robots continues to increase, the improvement in accuracy is no longer be obvious.

To illustrate the performance of the reliability check of the proposed RDCL algorithm, we add some measurement outliers at 200–300 epochs to simulate a fault. The proposed algorithm without NSS and the other algorithms are run with the same settings. The false alarm probability of NSS is 0.001. In horizontal position estimation, the degrees of freedom is 2. According to Fig. 5, the impact of measurement

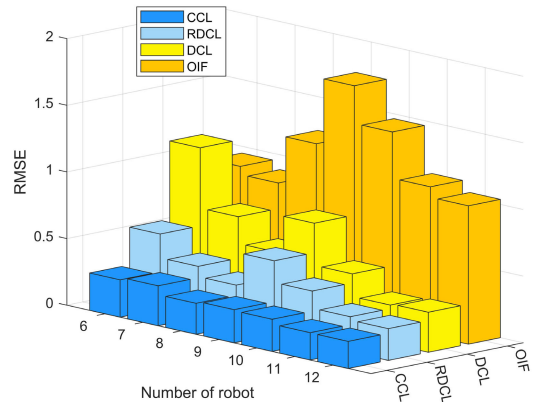


Fig. 4. RMSE versus the number of cooperating robots.

outliers on CCL, DCL, OIF, and RDCL algorithms without NSS is obvious. Furthermore, the position error of the DCL algorithm caused by sensor fault is up to nearly 6.5 m. The maximum position errors of OIF and RDCL algorithms without NSS are 4.6 and 3.2 m, respectively. Meanwhile, the CCL algorithm is able to recover from measurement anomalies

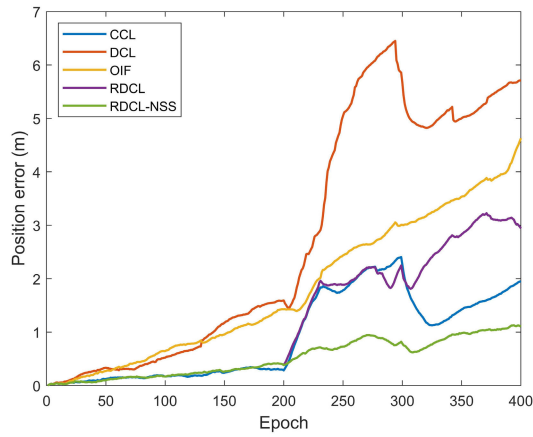


Fig. 5. Position error when increasing relative measurement error at 200–300 epochs.

as it requires a fusion center and measurement updates are globally communicated between all of the teammates. The performance of the proposed RDCL algorithm with NSS is better than that of the proposed algorithm without NSS and the CCL algorithm during a faulty period, and it improves the localization accuracy 58% and 44% compared with them. Furthermore, the proposed RDCL algorithm with NSS can detect and exclude the measurement fault effectively and significantly reduce position error.

B. Experiment

We compare the localization performance of the proposed RDCL algorithm with existing CL algorithms using the publicly available UTIAS multirobot CL and mapping dataset, where a fleet of five robots move in a rectangular indoor workspace with 15 landmarks [39]. Every robot is built from the iRobot Create platform and equipped with a netbook that interfaces with a monocular camera. The field of view of the monocular camera is about 60° . Meanwhile, cylindrical barcode tubes are installed on every landmark and robot. Wheel encoders mounted on the robot platform measure the linear and rotational angular velocities, while the monocular camera obtains range and bearing measurements when a barcode is detected. The ground-truth data, which includes the positions of landmarks and the Robot states, is monitored and logged by a Vicon motion capture system. This system provides a positional accuracy of the order of 1×10^{-3} m. The experimental platform and field are shown in Fig. 6.

To demonstrate the effectiveness and superiority of the proposed RDCL algorithm, we compare it to CCL, DCL, and OIF algorithms. The motion model is described by (4), and the discretization time is set as $\delta t = 0.02$ s. The measurement models between the robot and the landmark, as well as between robot and the other robot, are described by (5) and (6), respectively. The remaining parameters of these models are the same as those used in the simulation.

We compare the position errors of CCL, DCL, OIF, and RDCL algorithms using sub-dataset 1. The position errors of these algorithms for five mobile robots are illustrated in Fig. 7. The ARMSE of position, the ANEES, and the single step running time of the algorithms are given in Table III. Fig. 7 shows that the proposed RDCL algorithm has a smaller



Fig. 6. Experimental platform and field of the UTIAS multirobot CL dataset.

position error than the DCL and OIF algorithms. It has an average ARMSE of 0.68 m, which closely approximates the performance of the CCL algorithm (with an average ARMSE of 0.43 m), outperforming the DCL algorithm by 34%. Table III shows that the ANEES of the proposed algorithm is closer to those of the CCL and DCL algorithms. In contrast, the OIF algorithm, due to the neglect of the inter-robot correlations, has significantly different ANEES results compared with the three other algorithms. The experimental results of the OIF algorithm also suggest that the neglecting the inter-robot correlation leads to overly optimistic assessment of the estimation errors. Meanwhile, while the single step running time of the proposed RDCL algorithm exceeds that of the DCL and OIF algorithms, it remains lower than that of the CCL algorithm. Thus, the proposed RDCL algorithm not only improves localization accuracy but also exhibits favorable estimation consistency and computational efficiency.

To demonstrate the influence of the measurement errors on localization performance, we compare the localization performance of all of the algorithms under varying standard deviations of private and relative measurements. Fig. 8 shows the ARMSE of the position error when the standard deviation of the private measurement is set to $\sigma_p = 1:1:6$. The effect of standard deviation of private measurement on all of the algorithms is consistent, and the position errors of all of the algorithms increase as the standard deviations of private measurements increase; note that the position error of the RDCL algorithm is always the closest to that of the CCL algorithm. Fig. 9 shows the ARMSE of the position error when the standard deviation of relative measurement is set to $\sigma_r = 1:1:6$. It can be seen that the position errors of the DCL algorithm increase most significantly as the standard deviations of relative measurements increase. The position errors of OIF,

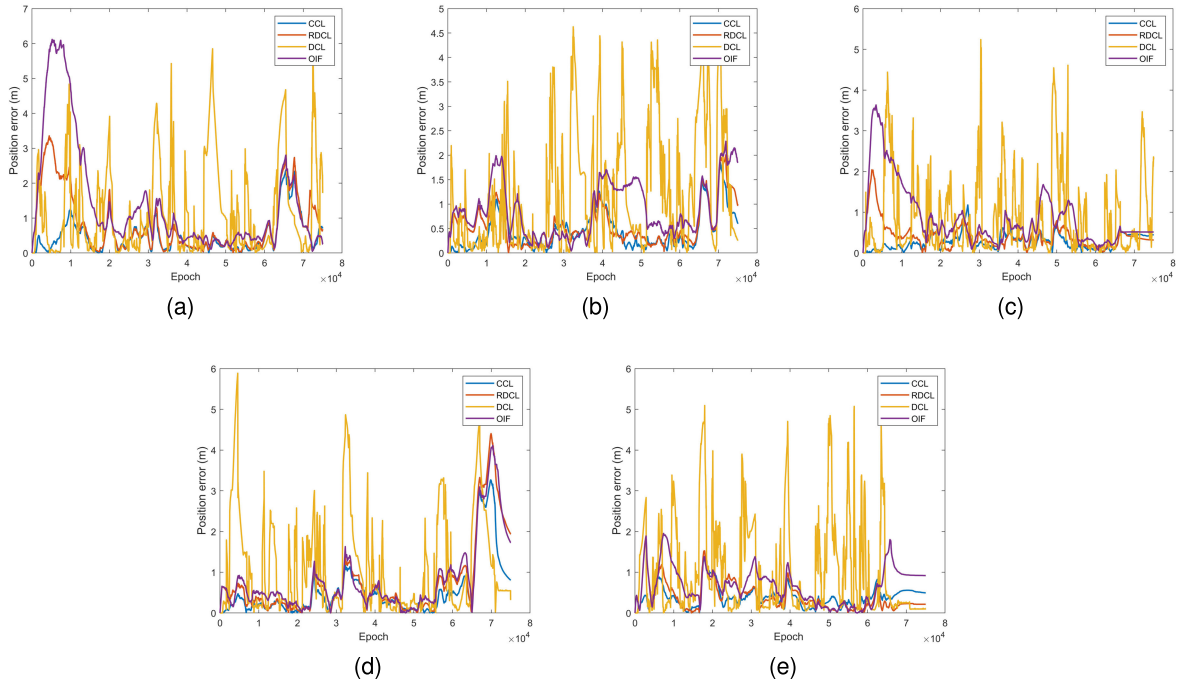


Fig. 7. Position errors of all of the algorithms for five robots. (a) Robot 1. (b) Robot 2. (c) Robot 3. (d) Robot 4. (e) Robot 5.

TABLE III
ARMSE OF POSITION, ANEES, AND RUNNING TIMES OF ALL OF THE ALGORITHMS FOR FIVE ROBOTS

Algorithm	Metrics	Robot 1	Robot 2	Robot 3	Robot 4	Robot 5
CCL	ARMSE (m)	0.48	0.47	0.29	0.51	0.38
	ANEES	42.83	60.91	32.55	46.33	34.67
	Time (s)	55.43	55.43	55.43	55.43	55.43
DCL	ARMSE (m)	1.21	1.24	0.83	1.03	0.95
	ANEES	39.15	262.45	32.10	55.77	31.47
	Time (s)	53.43	53.43	53.43	53.43	53.43
OIF	ARMSE (m)	1.79	1.03	1.03	0.77	0.68
	ANEES	679.64	293.91	3563.67	141.24	950.28
	Time (s)	50.53	50.53	50.53	50.53	50.53
RDCL	ARMSE (m)	0.91	0.91	0.45	0.72	0.40
	ANEES	102.39	83.11	63.86	68.97	39.69
	Time (s)	53.96	53.96	53.96	53.96	53.96

CCL, and RDCL algorithms increase slightly, but the proposed algorithm has the smallest errors. The results in Figs. 8 and 9 also show that either private measurement or relative measurement errors have the most impact on the localization performance of the DCL algorithm. This can be attributed to the fact that the private measurement updates and relative measurement updates of the DCL algorithm are executed sequentially, and the output of the private measurement updates serves as the input to the relative measurement updates. As the standard deviation of the relative measurement increases, the interference between measurement updates worsens, leading to degradation of the localization performance.

To show the impact of faulty landmark detection, we randomly associate a wrong ID with a landmark to observe the variation in position errors. Fig. 10 shows that faulty landmarks impair the localization performance of all of the algorithms. For the DCL algorithm, the measurement errors caused by the faulty landmarks affect not only the private

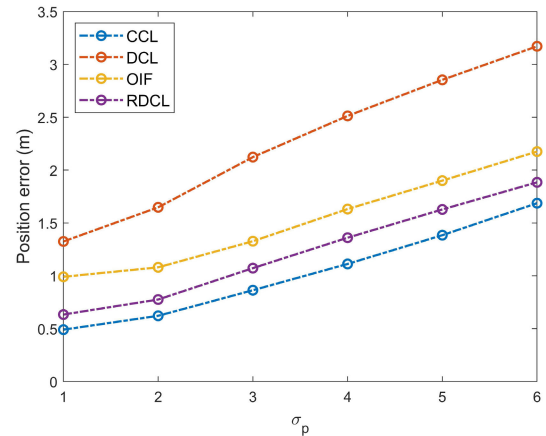


Fig. 8. Position error versus the standard deviation of the private measurement.

measurement update, but also the relative measurement update, resulting in the largest position errors. For the proposed

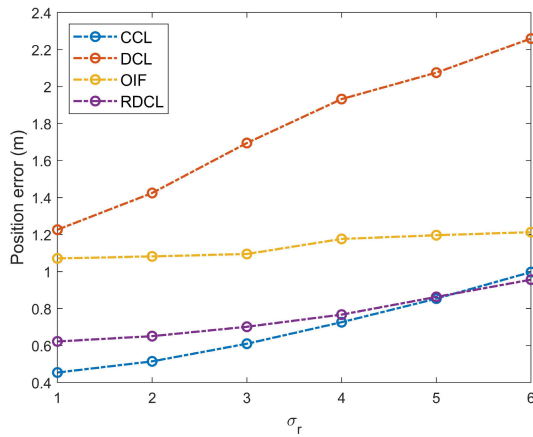


Fig. 9. Position error versus the standard deviation of relative measurement.

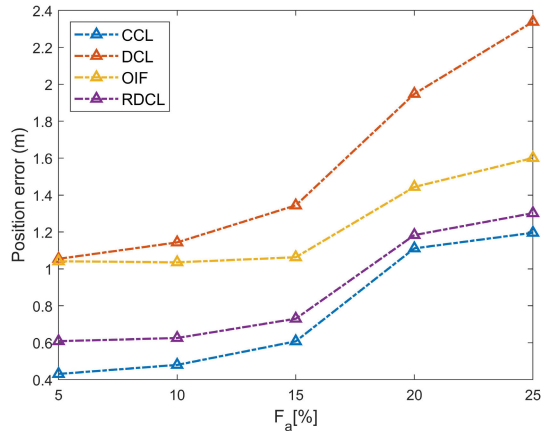


Fig. 10. Influence of faulty landmark associations on localization performance.

RDCL algorithm, the independence of the private and relative measurements avoids the effect caused by faulty landmarks. As the proportion of faulty landmarks increases, the localization accuracy of the proposed RDCL algorithm is always closest to that of the CCL algorithm.

V. CONCLUSION

In this article, a RDCL algorithm is proposed for multi-source multirobot systems. Compared to the traditional DCL algorithm, the proposed algorithm can track the dependencies for relative measurements; moreover, the private measurements are not involved in the cross correlation update and communication is limited to robots participating in the relative measurement update. The overall estimate of an individual robot is determined by the weighted sum of multisource estimates. Additionally, online validation makes the architecture robust and insensitive to measurement noise and outliers. Every robot recursively estimates only the latest state in a decentralized way, and the proposed algorithm is not restricted to specific models. This improvement makes the multirobot system an open architecture and more resilient. We compare the proposed algorithm with existing CL algorithms through simulations, and experiments using a real-world dataset. Simulation and experimental results show that the proposed RDCL algorithm has a better performance in terms of accuracy and resilience.

REFERENCES

- [1] A. Jahn, R. J. Alitappeh, D. Saldaña, L. C. A. Pimenta, A. G. Santos, and M. F. M. Campos, "Distributed multi-robot coordination for dynamic perimeter surveillance in uncertain environments," in *Proc. IEEE Int. Conf. Robot. Automat. (ICRA)*, Singapore, May 2017, pp. 273–278.
- [2] J. P. Queralta et al., "Collaborative multi-robot search and rescue: Planning, coordination, perception, and active vision," *IEEE Access*, vol. 8, pp. 191617–191643, 2020.
- [3] J. Alonso-Mora, E. Montijano, T. Nägele, O. Hilliges, M. Schwager, and D. Rus, "Distributed multi-robot formation control in dynamic environments," *Auton. Robots*, vol. 43, no. 5, pp. 1079–1100, Jun. 2019.
- [4] Y. Rizk, M. Awad, and E. W. Tunstel, "Cooperative heterogeneous multi-robot systems: A survey," *ACM Comput. Surv.*, vol. 52, no. 2, pp. 1–31, Apr. 2019.
- [5] Y. Huang, C. Xue, F. Zhu, W. Wang, Y. Zhang, and J. A. Chambers, "Adaptive recursive decentralized cooperative localization for multirobot systems with time-varying measurement accuracy," *IEEE Trans. Instrum. Meas.*, vol. 70, pp. 1–25, 2021.
- [6] L. R. Sahawneh and K. M. Brink, "Factor graphs-based multi-robot cooperative localization: A study of shared information influence on optimization accuracy and consistency," in *Proc. Int. Tech. Meeting Inst. Navigat. (ION ITM)*, Monterey, CA, USA, Mar. 2017, pp. 819–838.
- [7] P. Zhu and W. Ren, "Fully distributed joint localization and target tracking with mobile robot networks," *IEEE Trans. Control Syst. Technol.*, vol. 29, no. 4, pp. 1519–1532, Jul. 2021.
- [8] C. Tang, C. Wang, L. Zhang, Y. Zhang, and H. Song, "Multivehicle 3D cooperative positioning algorithm based on information geometric probability fusion of GNSS/wireless station navigation," *Remote Sens.*, vol. 14, no. 23, p. 6094, Dec. 2022.
- [9] B. Xu, S. Li, A. A. Razzaqi, Y. Guo, and L. Wang, "A novel measurement information anomaly detection method for cooperative localization," *IEEE Trans. Instrum. Meas.*, vol. 70, pp. 1–18, 2021.
- [10] S. S. Kia, S. F. Rounds, and S. Martinez, "A centralized-equivalent decentralized implementation of extended Kalman filters for cooperative localization," in *Proc. IEEE/RSJ Int. Conf. Intell. Robots Syst. (IROS)*, Chicago, IL, USA, Sep. 2014, pp. 3761–3766.
- [11] T. R. Wanasinghe, G. K. I. Mann, and R. G. Gosine, "Distributed leader-assistive localization method for a heterogeneous multirobotic system," *IEEE Trans. Autom. Sci. Eng.*, vol. 12, no. 3, pp. 795–809, Jul. 2015.
- [12] J. Zhu and S. S. Kia, "Cooperative localization under limited connectivity," *IEEE Trans. Robot.*, vol. 35, no. 6, pp. 1523–1530, Dec. 2019.
- [13] S. Wang, X. Jiang, and H. Wymeersch, "Cooperative localization in wireless sensor networks with AOA measurements," *IEEE Trans. Wireless Commun.*, vol. 21, no. 8, pp. 6760–6773, Aug. 2022.
- [14] G. P. Huang, N. Trawny, A. I. Mourikis, and S. I. Roumeliotis, "Observability-based consistent EKF estimators for multi-robot cooperative localization," *Auton. Robots*, vol. 30, no. 1, pp. 99–122, Jan. 2011.
- [15] P. Zhu, P. Geneva, W. Ren, and G. Huang, "Distributed visual-inertial cooperative localization," in *Proc. IEEE/RSJ Int. Conf. Intell. Robots Syst. (IROS)*, Xi'an, China, Sep. 2021, pp. 8714–8721.
- [16] T. R. Wanasinghe, G. K. I. Mann, and R. G. Gosine, "Distributed collaborative localization for a heterogeneous multi-robot system," in *Proc. IEEE 27th Can. Conf. Electr. Comput. Eng. (CCECE)*, Toronto, ON, Canada, May 2014, pp. 1–6.
- [17] E. D. Nerurkar, S. I. Roumeliotis, and A. Martinelli, "Distributed maximum a posteriori estimation for multi-robot cooperative localization," in *Proc. IEEE Int. Conf. Robot. Automat. (ICRA)*, Kobe, Japan, May 2009, pp. 1402–1409.
- [18] Y. Huang, Y. Zhang, B. Xu, Z. Wu, and J. A. Chambers, "A new adaptive extended Kalman filter for cooperative localization," *IEEE Trans. Aerosp. Electron. Syst.*, vol. 54, no. 1, pp. 353–368, Feb. 2018.
- [19] A. Miller, K. Rim, P. Chopra, P. Kelkar, and M. Likhachev, "Cooperative perception and localization for cooperative driving," in *Proc. IEEE Int. Conf. Robot. Automat. (ICRA)*, Paris, France, May 2020, pp. 1256–1262.
- [20] L. Luft, T. Schubert, W. Burgard, and S. I. Roumeliotis, "Recursive decentralized collaborative localization for sparsely communicating robots," in *Proc. Robot., Sci. Syst. (RSS)*, Ann Arbor, MI, USA, Jun. 2016.
- [21] S. I. Roumeliotis and G. A. Bekey, "Distributed multirobot localization," *IEEE Trans. Robot. Autom.*, vol. 18, no. 5, pp. 781–795, Oct. 2002.
- [22] S. S. Kia, J. Hechtbauer, D. Gogokhiya, and S. Martínez, "Server-assisted distributed cooperative localization over unreliable communication links," *IEEE Trans. Robot.*, vol. 34, no. 5, pp. 1392–1399, Oct. 2018.
- [23] L. C. Carrillo-Arce, E. D. Nerurkar, J. L. Gordillo, and S. I. Roumeliotis, "Decentralized multi-robot cooperative localization using covariance intersection," in *Proc. IEEE/RSJ Int. Conf. Intell. Robots Syst. (IROS)*, Tokyo, Japan, Nov. 2013, pp. 1412–1417.

- [24] T. Chang, K. Chen, and A. Mehta, "Resilient and consistent multi-robot cooperative localization with covariance intersection," *IEEE Trans. Robot.*, vol. 38, no. 1, pp. 197–208, Feb. 2022.
- [25] R. Jung, C. Brommer, and S. Weiss, "Decentralized collaborative state estimation for aided inertial navigation," in *Proc. IEEE Int. Conf. Robot. Automat. (ICRA)*, Paris, France, May 2020, pp. 4673–4679.
- [26] S. J. Julier and J. K. Uhlmann, "A non-divergent estimation algorithm in the presence of unknown correlations," in *Proc. Amer. Control Conf. (ACC)*, Albuquerque, NM, USA, Jun. 1997, pp. 2369–2373.
- [27] M. Reinhardt, B. Noack, P. O. Arambel, and U. D. Hanebeck, "Minimum covariance bounds for the fusion under unknown correlations," *IEEE Signal Process. Lett.*, vol. 22, no. 9, pp. 1210–1214, Sep. 2015.
- [28] L. Luft, T. Schubert, S. I. Roumeliotis, and W. Burgard, "Recursive decentralized localization for multi-robot systems with asynchronous pairwise communication," *Int. J. Robot. Res.*, vol. 37, no. 10, pp. 1152–1167, Sep. 2018.
- [29] R. Jung and S. Weiss, "Scalable recursive distributed collaborative state estimation for aided inertial navigation," in *Proc. IEEE Int. Conf. Robot. Automat. (ICRA)*, Xi'an, China, May 2021, pp. 1896–1902.
- [30] P. Yang, D. Duan, C. Chen, X. Cheng, and L. Yang, "Multi-sensor multi-vehicle (MSMV) localization and mobility tracking for autonomous driving," *IEEE Trans. Veh. Technol.*, vol. 69, no. 12, pp. 14355–14364, Dec. 2020.
- [31] M. Mukherjee, A. Banerjee, A. Papadimitriou, S. S. Mansouri, and G. Nikolakopoulos, "A decentralized sensor fusion scheme for multi sensorial fault resilient pose estimation," *Sensors*, vol. 21, no. 24, p. 8259, Dec. 2021.
- [32] C. Tang, Y. Wang, L. Zhang, Y. Zhang, and H. Song, "Multisource fusion UAV cluster cooperative positioning using information geometry," *Remote Sens.*, vol. 14, no. 21, p. 5491, Oct. 2022.
- [33] Q. Meng and L. Hsu, "Resilient interactive sensor-independent-update fusion navigation method," *IEEE Trans. Intell. Transp. Syst.*, vol. 23, no. 9, pp. 16433–16447, Sep. 2022.
- [34] J. Al Hage, M. E. El Najjar, and D. Pomorski, "Multi-sensor fusion approach with fault detection and exclusion based on the Kullback–Leibler divergence: Application on collaborative multi-robot system," *Inf. Fusion*, vol. 37, pp. 61–76, Sep. 2017.
- [35] M. Wu, H. Ma, and X. Zhang, "Decentralized cooperative localization with fault detection and isolation in robot teams," *Sensors*, vol. 18, no. 10, p. 3360, Oct. 2018.
- [36] S. Fang, H. Li, and M. Yang, "LiDAR SLAM based multivehicle cooperative localization using iterated split CIF," *IEEE Trans. Intell. Transp. Syst.*, vol. 23, no. 11, pp. 21137–21147, Nov. 2022.
- [37] A. Howard, M. J. Mataric, and G. S. Sukhatme, "Putting the 'I' in 'team': An ego-centric approach to cooperative localization," in *Proc. IEEE Int. Conf. Robot. Automat.*, Taipei, Taiwan, Sep. 2003, pp. 868–874.
- [38] H. Li and F. Nashashibi, "Cooperative multi-vehicle localization using split covariance intersection filter," *IEEE Intell. Transp. Syst. Mag.*, vol. 5, no. 2, pp. 33–44, Summer 2013.
- [39] K. Y. Leung, Y. Halpern, T. D. Barfoot, and H. H. Liu, "The UTIAS multi-robot cooperative localization and mapping dataset," *Int. J. Robot. Res.*, vol. 30, no. 8, pp. 969–974, Jul. 2011.



Dongjia Wang received the B.S. degree in electronic science and technology from the Xi'an University of Science and Technology, Xi'an, China, in 2012, and the M.S. degree in communication and information systems from Xidian University, Xi'an, in 2016. He is currently pursuing the Ph.D. degree in information and communication engineering with Northwestern Polytechnical University, Xi'an.

His research interests include visual navigation, integrated navigation, and collaborative navigation.



Huaiyuan Qi received the B.S. degree in communication engineering from Northwestern Polytechnical University, Xi'an, China, in 2005.

He is currently a Senior Engineer with Shaanxi Fenghuo Electronics Company Ltd., Baoji, China. His research interests include wireless positioning and emergency rescue.



Baowang Lian received the Ph.D. degree in information and communication engineering from Northwestern Polytechnical University, Xi'an, China, in 2006.

He is currently a Professor with the School of Electronics and Information, Northwestern Polytechnical University. His research interests include satellite navigation, visual navigation, integrated navigation, and collaborative navigation.



Yangyang Liu received the Ph.D. degree in information and communication engineering from Northwestern Polytechnical University, Xi'an, China, in 2020.

He is currently a Research Associate with the School of Electronics and Information, Northwestern Polytechnical University. His research interests include cooperative navigation and integrated navigation.



Houbing Song (Fellow, IEEE) received the Ph.D. degree in electrical engineering from the University of Virginia, Charlottesville, VA, USA, in August 2012.

He is currently a tenured Associate Professor and the Director of the Security and Optimization for Networked Globe Laboratory (SONG Lab, www.SONGLab.us), University of Maryland, Baltimore County (UMBC), Baltimore, MD, USA. Prior to joining UMBC, he was a tenured Associate Professor of electrical engineering and computer science

with Embry-Riddle Aeronautical University, Daytona Beach, FL, USA. He is an editor of eight books, the author of more than 100 articles, and an inventor of two patents. His research interests include cyber-physical systems/the Internet of Things, cybersecurity and privacy, and AI/machine learning/big data analytics. His research has been sponsored by federal agencies (including the National Science Foundation, U.S. Department of Transportation, and Federal Aviation Administration) and industry. His research has been featured by popular news media outlets, including IEEE GlobalSpec's Engineering360, Association for Uncrewed Vehicle Systems International (AUUSI), Security Magazine, CXOTech Magazine, Fox News, U.S. News and World Report, The Washington Times, and New Atlas.

Dr. Song is an ACM Distinguished Member and an ACM Distinguished Speaker. He is a Highly Cited Researcher identified by Clarivate in 2021 and 2022 and a Top 1000 Computer Scientist identified by Research.com. He has received the Research.com Rising Star of Science Award in 2022 (World Ranking: 82 and U.S. Ranking: 16). He was a recipient of more than ten Best Paper Awards from major international conferences, including IEEE International Conference on Cyber, Physical and Social Computing (CPSCom) in 2019, IEEE International Conference on Industrial Internet (ICII) in 2019, IEEE/American Institute of Aeronautics and Astronautics (AIAA) Integrated Communications Navigation and Surveillance Conference (ICNS) in 2019, IEEE International Conference on Cloud and Big Data Computing (CBD-Com) in 2020, International Conference on Wireless Algorithms, Systems, and Applications (WASA) in 2020, AIAA/IEEE Digital Avionics Systems Conference (DASC) in 2021, IEEE Global Communications Conference (GLOBECOM) in 2021, and IEEE International Conference on Computer Communications (INFOCOM) in 2022. He was an Associate Technical Editor of *IEEE Communications Magazine* from 2017 to 2020. He has been serving as an Associate Editor for IEEE INTERNET OF THINGS JOURNAL since 2020, IEEE JOURNAL ON MINIATURIZATION FOR AIR AND SPACE SYSTEMS (J-MASS) since 2020, IEEE TRANSACTIONS ON INTELLIGENT TRANSPORTATION SYSTEMS since 2021, and IEEE TRANSACTIONS ON ARTIFICIAL INTELLIGENCE (TAI) since 2023.